Physio-Mechanical and Petrographic Characteristics of Granitic Rocks from the Demote Valley, Gilgit, Pakistan: Implications for Strength and Bearing Capacity.

Shahbaz Alam[1], Masroor Alam[1*], Ishfaq Ahmad[2,3*], Sona karim[4,3], Massam Ali[5,3], Meixia Zhao[2], Muhib Ullah[6], Shaikh Sanaullah[7,3], Amjad Ali[8], Izhar Ahmed[9,3]

[1]Karakoram International University, Gilgit, 15100, Pakistan

[2]Key Laboratory of Ocean and Marginal Sea Geology, South China Sea Institute of Oceanology, Chinese Academy of Sciences, Guangzhou,510301, China

[3]University of Chinese Academy of Sciences, Beijing, 100049, China

[4]State Key Laboratory of Desert and Oasis Ecology, Key Laboratory of Ecological Safety and Sustainable Development in Arid Lands, Xinjiang Institute of Ecology and Geography, Chinese Academy of Sciences, Urumqi, 830011, China

[5]State Key Laboratory of Ore Deposit Geochemistry, Institute of Geochemistry, Chinese Academy of Sciences, Guiyang, China

[6]Center for Geographical Information System, University of the Punjab, Lahore, 54590, Pakistan

[7]State Key Laboratory of Tropical Oceanography, South China Sea Institute of Oceanology, Chinese Academy of Sciences. Guangzhou, 510301, China

[8]School of earth science and resources, China University of Geosciences, Beijing

[9]Key Laboratory of Shale Gas and Geoengineering (KLSGG), Institute of Geology and Geophysics, Chinese Academy of Sciences, Beijing, 100029, China

*__Correspondence__: masroor.alam@kiu.edu.pk, ahmadishfaq54726@gmail.com

The granitic rocks of the Damote Valley (Juglote Group, Kohistan Batholith) were evaluated for their physio-mechanical and petrographic properties to assess their suitability for construction, particularly as dimension stones. Detailed petrography and tests such as Uniaxial Compressive Strength (UCS), Brazilian Tensile Strength (BTS), Ultrasonic Pulse Velocity (UPV), Schmidt Hammer, Specific Gravity, Porosity, Water Absorption, and Slake Durability were conducted. The granitic rocks, medium to coarse-grained with no preferred orientation, consist mainly of plagioclase (19–35%), quartz (30–43%), and alkali feldspar (40–44%), along with biotite, muscovite, sericite, and minor opaque minerals. Based on geographic location, the granites are divided into three zones: Fulkin granite (Zone 1), Bargin (Zone 2), and Shing (Zone 3). The average Uniaxial Compressive Strength (UCS) values of the granite from the Demote area are 63 MPa for Fulkin granite, 66 MPa for Bargain granite, and 53 MPa for Shing granite, reflecting the granite's suitability for engineering applications. BTS values range from 7.55 to 12.04 MPa. Schmidt hammer rebound values range from 43 to 47, while specific gravity averages from 2.5 to 2.98. Water absorption is low (0.34–0.60%), and porosity ranges from 1.19% to 1.28%. All results fall within ASTM specifications. The medium-grained granite is stronger and more durable than coarse-grained varieties due to its tighter grain packing and fewer microcracks. Based on these findings, Damote granites are suitable for construction in roads, bridges, constructions, and the dimension stone in the area.

Keywords: Granitic Rocks, Physio-Mechanical Properties, Petrography, Gilgit Baltistan.

Introduction:

Pakistan is one of the countries with significant granitic rock formations, particularly in the northern part [1]. These formations are part of extensive geological belts stretching through the Himalayas and Trans-Himalayas [2][3][4]. These granitic formations in northern Pakistan are commonly used as dimension and building stones. Their suitability for construction is significantly affected by various properties, which are shaped by factors like the conditions during rock formation, subsequent metamorphic processes, and tectonic activity. Several research papers have been published focusing on the granitic rocks in this region [1], [5][6][7][8][9][10]. Approximately 90% of studies have concluded that granitic rocks in this region are highly suitable for construction purposes [6][11]. Due to their strength and durability, these rocks are widely used in masonry buildings, road construction, dams, and tunnels [6].

The physio-mechanical properties of rocks used as building and dimension stones are widely discussed in the literature [12][13][14]. These properties are influenced by various factors, though the mechanical behavior of the rock resulting from many elements, such as petrography, mineralogy, textural features, weathering, porosity, and the presence of fissures [15][16][17][18]. As granitic rocks are used as building materials, the construction industry aims to meet all physical and mechanical requirements to ensure their suitability. Also understanding the behavior and nature of these rocks necessitates careful consideration of petrographic elements, such as cracks, grain orientation, size, and contour [19]. For example, the Kumrate granite near the study area has been examined for its petrographic and mechanical characteristics, revealing properties that make it suitable for construction [20].

Objectives and Novelty:

`Despite extensive research on granitic rocks in northern Pakistan, the geotechnical and mechanical behavior of rocks in the Damote Valley, particularly in the northwestern region, remains underexplored, highlighting the need for further investigation to understand their engineering properties and potential applications in construction. Given the multitude of factors influencing the geotechnical properties of granitic rocks, this research seeks to address the primary question: 'How do the physical, mechanical, and petrographic properties of granitic rocks be used to assess their viability as dimension stones and construction materials?' Another question we interrogate is 'What specific characteristics make granitic rocks suitable or unsuitable for construction purposes.

Tectonic and Geological Setting of the Area:

Gilgit Baltistan (GB) situated within the Northern Area district of Pakistan, is bordered by Afghanistan to the west, the Indian Ladakh region to the east and southeast, and China (Xinjiang and Tibet) to the north and far east. The region experiences significant seismic activity due to the collision of the Indian and Eurasian plates, resulting in intra-oceanic subduction during the Cretaceous period, formation of volcanic arcs including the Kohistan Island Arc (KIA) and Ladakh Island Arc (LIA) [21][22]. These island arcs collided with the Eurasian Plate along the Shayok Suture, resulting in the formation of the Main Karakorum Thrust (MKT) [23][24], while the collision of the Indian plate with Kohistan and Ladakh during the Eocene led to the Main Mantle Thrust (MMT) [22]. The KIA, resulting from the subducted Tethyan crust within the Eurasian domain, has created the distinct Nanga-Parbat Syntaxes (NPS). Regional earthquakes are primarily associated with regional faults and local stress zones. Cenozoic magmatism in the KIA, represented by Sharman volcanics in northern Kohistan and Dir-Utror volcanics in the southwestern region [25], later underwent intrusion by stage-2 plutons (granodiorites and granites) from the Kohistan batholith [23]. The Dir group in the southwestern Kohistan arc forms a gently folded belt approximately 120 km long and 10-15 km wide, extending from the upper Swat Valley into Dir [26]. Transitioning through the Lamutai region, the granitic rocks of the Kumrat Valley and Tall area, consist of stage-2 plutons that intrude Utror volcanic [23].

The study area, Damote Valley, is characterized as a V-shaped valley predominantly composed of the Juglote Group of rocks, which cover metasediments and metavolcanic (Figure 1). This group is further intruded by various lithologies, including paragneiss, schist, amphibolite, granite, and calc-silicate rocks [9].
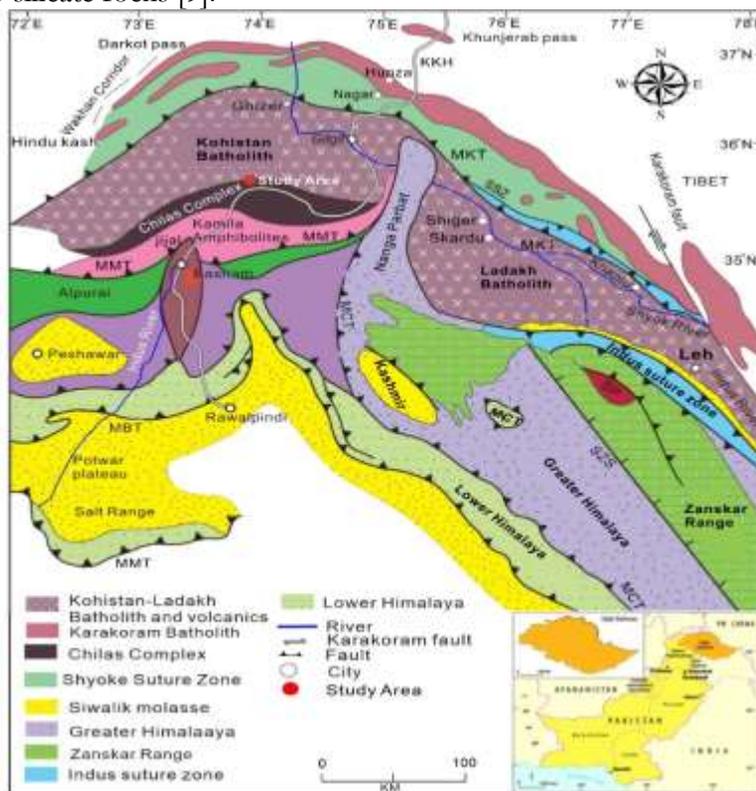
Figure 1. Geological map of the Kohistan Island Arc (KIA), modified from [27]. The study area is indicated by the red circle on the map.

Materials and Methods:

To achieve the desired goals, the following method was used, as shown in (Figure 2). This study incorporated an organized and systematic procedure that includes several steps.
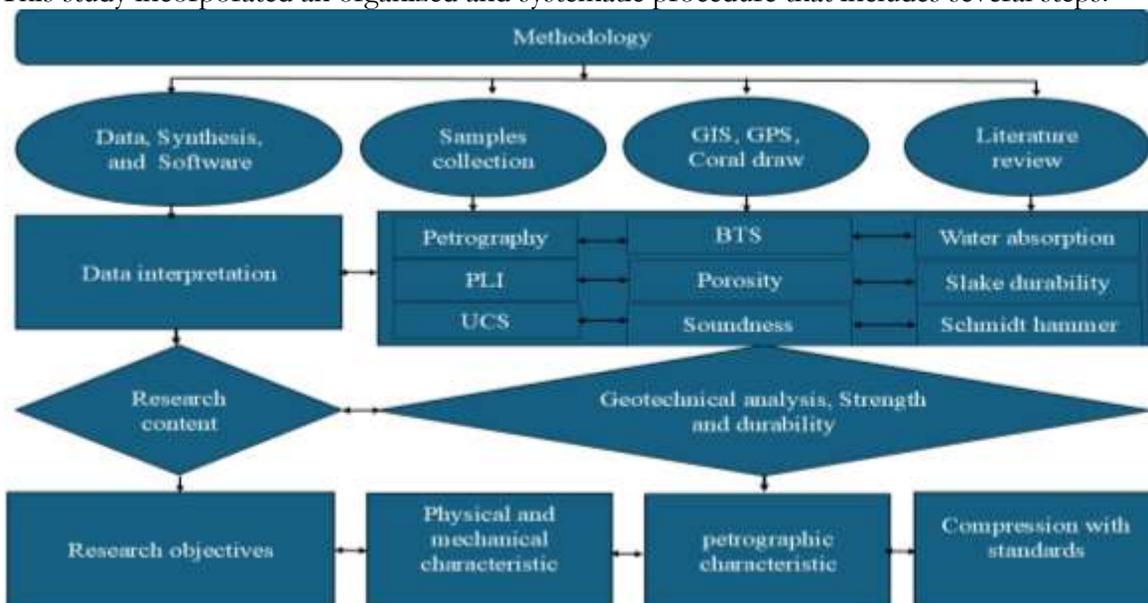
Figure 2. Flowchart outlining the process of data collection, laboratory testing, and result interpretation.

Field Surveys and Data Collection:

The study area located is in the Damote Valley district of Gilgit which is extended to almost 500 m. Rock samples were collected from the following geographic coordinates: 35° 40' 48" N, 74° 34' 59" E (Z1); 35° 40' 59" N, 74° 34' 45" E (Z2); and 35° 40' 25" N, 74° 34' 20" E (Z3). The area is well accessible and almost all samples' localities are along roadsides (Figure 3). Nine bulk samples of Granite, three from each locality (3x3=9) were collected. For details of sample collection see Table 1.

Figure 3. Showing field photography of the study area Demote granite.

Table 1. Details of sample collection, including location, sample name, geological unit, sample abbreviations, and grain size of the granitic rock.

Location	Sample name	Geological unit	Sample abbreviations	Grain size
Fulkin (Z1)	Fulkin Granite	Kohistan Batholith	FG- 1	Coarse to very coarse grain
Fulkin (Z1)	Fulkin Granite	Kohistan Batholith	FG- 2	Coarse to very coarse grain
Fulkin (Z1)	Fulkin Granite	Kohistan Batholith	FG- 3	Coarse to very coarse grain
Shing (Z2)	Shing Granite	Kohistan Batholith	SG- 1	Coarse to very coarse grain
Shing (Z2)	Shing Granite	Kohistan Batholith	SG- 2	Coarse to very coarse grain
Shing (Z2)	Shing Granite	Kohistan Batholith	SG- 3	Coarse to very coarse grain
Bargain (Z3)	Bargain Granite	Kohistan Batholith	BG- 1	Coarse to very coarse grain
Bargain (Z3)	Bargain Granite	Kohistan Batholith	BG- 2	Coarse to very coarse grain
Bargain (Z3)	Bargain Granite	Kohistan Batholith	BG- 3	Coarse to very coarse grain

Laboratory Test:

The samples are prepared by the Department of Mining Engineering Karakorum International University Gilgit Baltistan. The sample cores were made by ASTM specifications (Figure 4a). To detail mechanical, physical, and petrography tests are mentioned below research. These core samples were cut and ground into the necessary size by ASTM standards [28]. For all tests conducted in this study, a total of three replicates were tested for each granite type to ensure accuracy and repeatability. The results were averaged across the replicates to provide a mean value for each granite type. For the Schmidt Hammer Rebound and Ultrasonic Pulse Velocity (UPV) tests, multiple measurements were taken at different locations on each granite sample, and the averages of these measurements were used. Similarly, for the physical properties (e.g., water absorption, specific gravity, and porosity), three replicate measurements were made, and the mean value was calculated for each property.

For the UCS test, The ASTM-C170-90 and ASTM-D2938 requirements were followed in the preparation of the cylinders by cutting and grinding the cores (Figure 4b). After aligning the core samples perpendicularly, the UCS test was conducted by applying a load at a rate of 0.2 MPa/sec until the samples failed (see Figure 4c). Similarly, the BTS test is performed to obtain the tensile strength of the rock. The direct determination of BTS is difficult and it is too hard to grip samples between the load plates of the testing machine so BTS seems to be a simple alternative to evaluate tensile strength. According to ASTM standards (ASTM-D3976), Cores were cut to a thickness-to-diameter ratio of at least 0.2 to 0.5 to complete the Brazilian tensile test. After that, the discs were put into the machine and tested (Figure 4d).

The Schmidt hammer, a non-destructive tool, was utilized to evaluate the hardness of the rocks. To correlate these measurements with UCS (Uniaxial Compressive Strength) values, readings were also taken from intact granite samples collected from representative areas (Figure 5a and 5b). It was make sure to take rebound numbers from smooth and new surfaces using the ASTM recommended because fractured and rough surfaces can alter rebound values [29]. The test UPV is also performed to find homogeneity, the presence of cracks, and void space in a rock (Figure 5f). The Slake Durability Test is then performed to assess the resistance of coarse aggregates in the rock. Before testing, samples weighing between 400 and 600 grams must be dried at 105±5 degrees Celsius. The samples were placed in a drum filled with water and subjected to a maximum speed of 20 revolutions per minute for 10 minutes. After this period, the samples are removed and placed in an oven for an additional 10 minutes, after which their weight is recorded again (w2) for accurate calculation. The Slake Durability Index is calculated using the formula 1.

$$\text{Slake Durability index } = \frac{A-D}{C-D} \times 100 \qquad (2)$$

Where,

A = weight of the sample after the first cycle,

C = weight of the sample after the second cycle,

D = initial dry weight of the sample,

(A−D) = weight loss after the first cycle,

(C−D) = weight loss after the second cycle.

The percent loss of mass is referred to as the slake durability index.

Several tests were performed to assess the physical properties of granite samples, focusing on water content, which is crucial for evaluating their durability in engineering applications. To determine water absorption. We submerged the samples in water for 48 hours, weighed them, and then dried them in an oven at 60°C for another 48 hours before weighing them again to calculate the water absorption (Figure 5a). and calculating water content (W) using the formula 2.

$$W = \frac{Ww - Wd}{Wd} \times 100 \qquad (2)$$

Where,

WW = Weight of the saturated sample

Wd = weight of the dried sample.

We also determined the specific gravity of the rock samples, which is important for evaluating their suitability as building stones. This was done by weighing the rock aggregate, submerging it in water for 24 hours, and reweighing it in air while saturated (Figure 5b).

Micro-fractures, void spaces, and pores in rocks can adversely affect their strength properties. Rocks with a high number of pores or voids tend to have decreased durability and are more susceptible to physical weathering. Factors such as grain size, shape, mineralogical arrangement, and the percentage of clay minerals play a significant role in controlling rock porosity [18]. The porosity of the granite in the study area was determined by the formula 3.

$$P = \frac{Wt.\,in\,Air - DryWt.}{Wt.\,in\,Air - (Wt.in\,Water)} \times 100 \qquad (3)$$

soundness test was carried out per ASTM C 88-90 (2003) to analyze the rocks' resistance to chemical weathering and their durability against environmental factors, including temperature variations, dryness, moisture content, and saline water (Figure 5c).
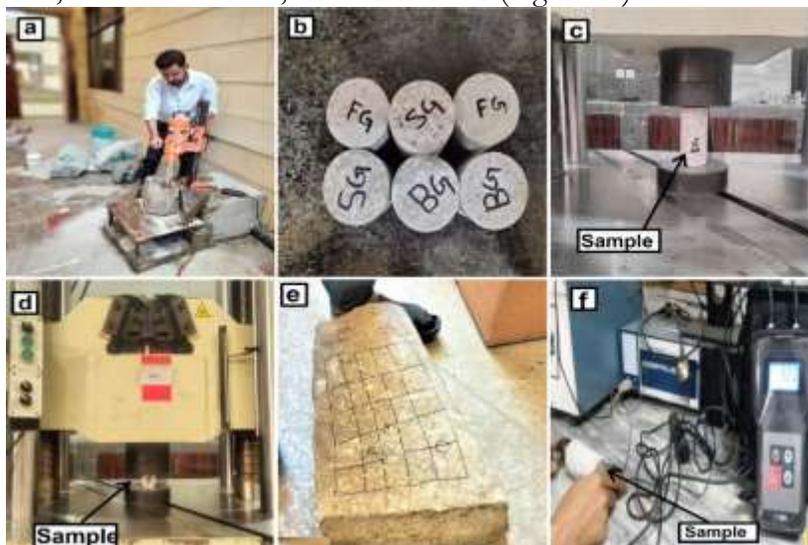
Figure 4. a) Core drilling with required disc size, b) Preparation of core cylinders for UCS testing, c) Crushing core samples in the UTM machine, d) Brazilian test conducted on discs in the UTM machine, e) Marking lines for rebound value measurements, f) UPV test

Results Petrography:

The petrographic analysis in this study is based on field observations of key geological features, coupled with an in-depth microscopic examination of representative granite samples. These samples were analyzed under plane-polarized light (PPL) and cross-polarized light (XPL) in the petrography lab at the National Centre of Excellence in Geology (NCEG) Peshawar. The study focuses on factors influencing the engineering properties of granite, including microfractures, mineral alteration, sericitization, and mineral texture.

The Damote granite displays a texture that ranges from sub-equigranularity to inequigranular, without any preferential orientation. Table 2 outlines the model mineralogical composition of the study area, highlighting key minerals such as quartz, alkali feldspar, plagioclase, and mica (including muscovite and biotite). Secondary minerals include apatite and opaque minerals, while chlorite and sericite are present as accessory minerals. The model's essential minerals are plotted on the IUGS classification diagram, which illustrates that the studied samples fall within the granite compositional field (Figure 6).

Figure 5. a) Weighing in water procedure, (b) Aggregates dipped in water as per ASTM standards, (c) Demonstrating the soundness test procedure for granite rock aggregates, with samples immersed in a water vessel containing MgSO₄ solution.
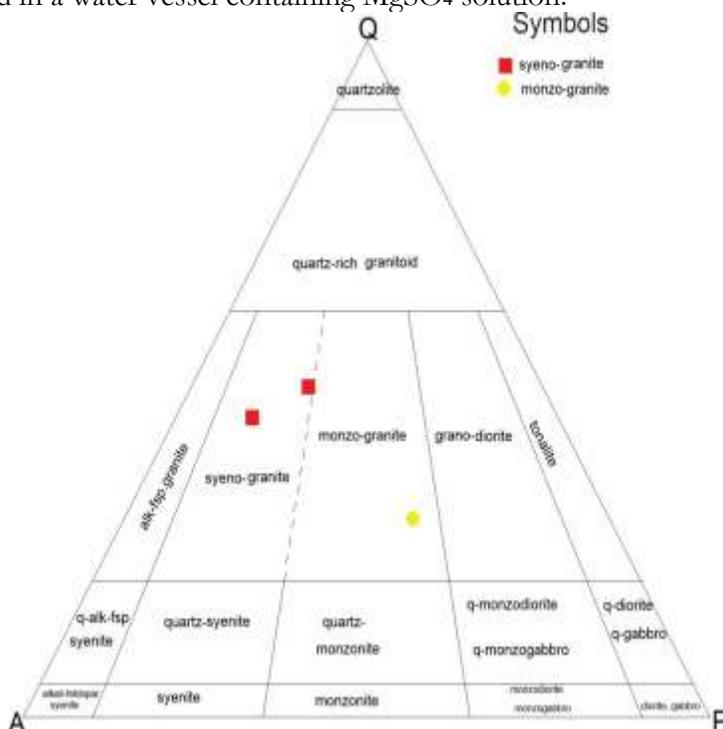
Figure 6. The modal composition of the Damote granitic rocks is plotted on the IUGS classification diagram, as modified after [30].

The modal mineralogical study of quartz in the Damote granite reveals a range of 43% to 25%, based on microscopic observations. Quartz occurs as medium to coarse-sized, anhedral to subhedral grains, with approximately 17% of the grains exhibiting strain, characterized by

undulose extinction. The presence of strained quartz grains offers insights into the extent of deformation within the Damote granite (Figure 7a). Unstrained quartz grains, in contrast, are rarely observed in the studied samples.

The second most abundant mineral in the Damote granite is potassium feldspar, which ranges from 40% to 20%, with microcline being the predominant form (20%) (Table 2). Some feldspar grains contain inclusions of other minerals, such as biotite and opaque minerals, resulting in a poikilitic texture (Figure 7b). Also, some alkali feldspar grains display a myrmakitic texture (Figure 7c). All alkali feldspar grains are subhedral to euhedral in shape, with some containing inclusions of other minerals, contributing further to the poikilitic texture.

The modal mineral content of plagioclase ranges from 15% to 30% (Table 2). Typically, plagioclase occurs as subhedral to euhedral grains (Figures 7d and 7h). While some grains exhibit Carlsbad and albite polysynthetic twinning, most display zoning (Figures 7g and 7h). Muscovite abundance ranges from 8% to 10% (Table 2), appearing as medium-sized, fully developed flakes with dark green to light green pleochroism (Figures 7e and 7h). Quartz and opaque minerals, such as chlorite, are often associated with biotite (Figure 7h).
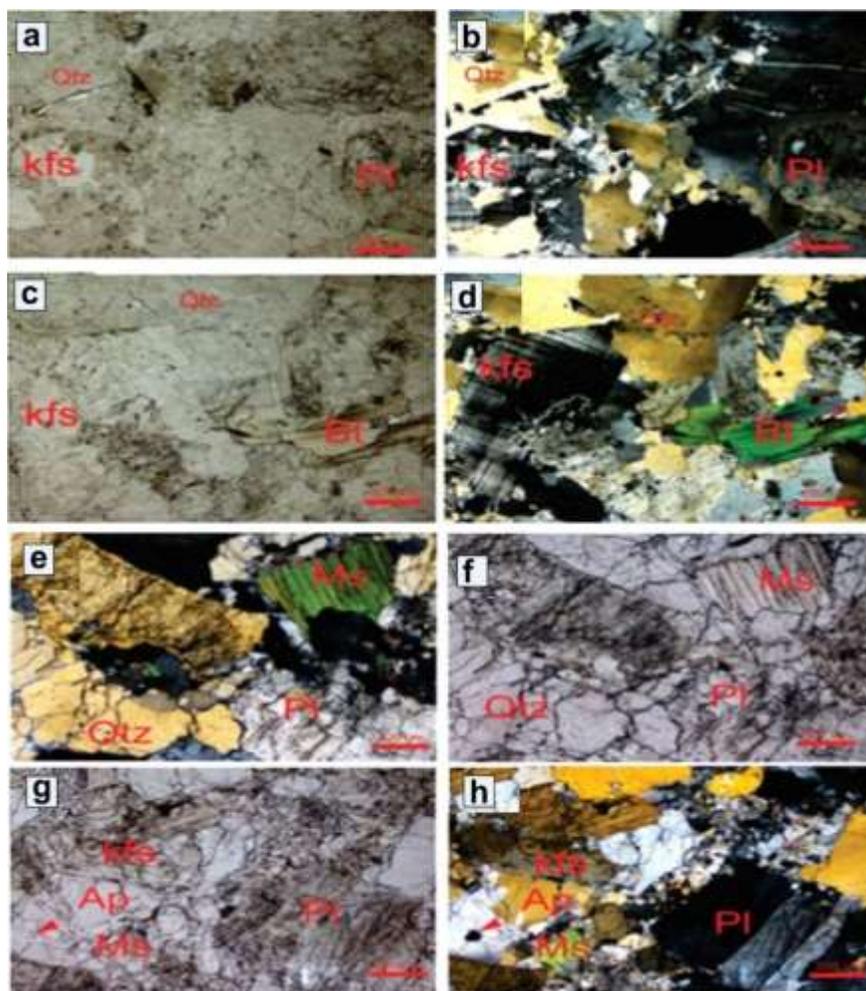
Figure 7. Photomicrograph showing the petrographic features of Demote granites: (a) Strained quartz indicating deformation, (b) Inclusions forming a poikilitic texture, (c) Alkali feldspar exhibiting a myrmakitic texture, (d) Twinned grains with zoning, subhedral-euhedral, (e) Zoning in plagioclase grains, subhedral-euhedral, (f) Carlsbad and albite polysynthetic twinning in some grains, (g) Pleochroism from dark green to light green, (h) Association of quartz, chlorite, and opaque minerals with biotite

Table 2 Mineralogical composition model of the Demote granitic rocks

Minerals	Coarse-grained granite			Medium grained granite		
Quartz Alkali feldspar	43	35	25	30	25	19
	40	20	30	33	44	38
Plagioclase	15	10	19	30	15	35
Muscovite	8	4	7	10	7	5
Biotite	8	5	4	5	7	6
Chlorite	1.3	4.5	1.7	1.4	3.8	1.6
Apatite Sericite	0.4	0.3	0.5	0	0	0.3
	1	2	1	1.3	3.4	1.3
Opaque	0.5	1.5	1.8	2.9	3.7	1.5

Mechanical Properties:

Unconfined Compressive Strength (UCS):

The highest UCS value was recorded for Bargain granite (BG) at 66.17 MPa, while the lowest was recorded for Shing granite (SG) at 53.22 MPa. The UCS value for Fulkin granite was recorded as 63.10 MPa. Based on rock classification and petrographic properties, medium to coarse-grained granites are classified as moderately strong to strong, according to [31]. According to Brady and Brown [32] UCS values for granitic varieties are approximately 6–11 times higher than UTS values. Therefore, UCS can serve as an index property to evaluate granite's suitability as a dimension stone, providing resistance across nearly all physio-mechanical and petrographic characteristics [33]. Figure 8a illustrates the UCS results graphically, and the average UCS values are presented in Table 3.
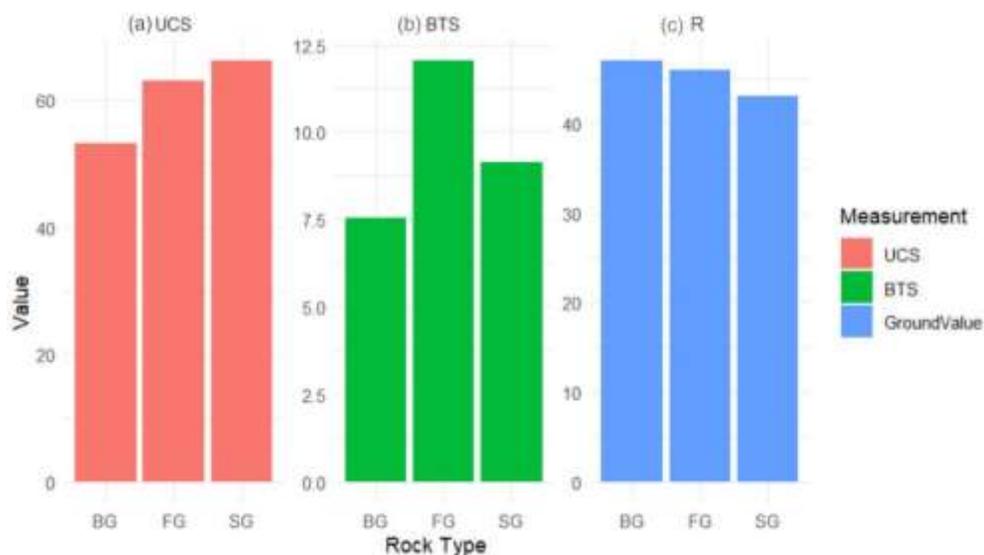
Figure 8. Average Results of a) Uniaxial Compression Strength (UCS), b) Brazilian Tensile Strength (BTS), and c) Schmidt Hammer Rebound Test (R)

Brazilian Tensile Strength (BTS):

The highest BTS value was observed in Bargain granite (BG) at 12.04 MPa, while the lowest mean value was noted in Shing granite (SG) at 7.55 MPa. According to BTS measurements, all granite types meet the ASTM requirements ($\geq$8.27 MPa) for use as dimension and building stone. The BTS results are shown in Figure 8b, and the average results are presented in Table 3.

Schmidt Hammer Test:

During in-situ field observations, non-destructive Schmidt hammer rebound values were measured at various locations in the study area. A minimum of 10 rebound values was taken for

each sample, and the averages were calculated. Bargain granite (BG) exhibited the highest Schmidt hardness value (47) among the intact rocks, while Fulkin granite and Shing granite showed lower Schmidt hardness values than Bargain granite (see Table 3). Figure 8c provides a graphical representation of these results.

Ultrasonic Pulse Velocity:

Dried core cylinders were tested for ultrasonic pulse wave velocity. Fulkin granite showed a mean velocity of 2811.40 m/s, while Shing granite (SG) recorded the highest velocity at 3228.62 m/s. UPV values closely correlate with the strength of granites and generally follow the same trend as UCS, they can potentially serve as an index feature for evaluating granite quality. Table 3 presents the average UPV results.

Slake Durability:

The slake durability test was conducted to determine the resistance of rock samples to weakening and disintegration when subjected to two standard cycles of drying and wetting in a slaking fluid, usually water. Fulkin Granite (FG) exhibited the highest value at 37.5, while Shing Granite (SG) recorded the lowest value at 35.6, and Bargain Granite (BG) had a value of 36.2. According to IS-10050-1981, the maximum standard value should be less than 40%. The detailed average results of the slake durability test are provided in Table 3.

Table 3 Average mechanical test results (UCS, BTS, R, UPV, and Ground Value) obtained from laboratory analysis.

Rock ID	Average UCS (MPa)	Average BTS (MPa)	Average Schmidt Hammer (R)	Average UPV (m/s)	Average Slake Durability
FG	63.10	12.04	46	2,811.40	37.5
SG	66.17	9.15	43	2957.03	35.6
BG	53.22	7.55	47	3,218.60	36.2

Physical Properties:

Water Absorption:

Fulkin Granite (FG) recorded the highest water absorption value at 0.60%, while Bargen Granite (BG) exhibited the lowest average value of 0.34% (see Table 4). According to ASTM C97/C97M, Fulkin Granite (FG), Shing Granite (SG), and Bargen Granite (BG) meet the criteria for use as dimension or construction stone, as their water absorption values are below 0.4%. Generally, ASTM recommends that rocks with water absorption below 2% are acceptable. Although Fulkin Granite (FG) has a mean value slightly above the ASTM recommendation, specimens SG (0.45%) and BG (0.34%) fall within the specified range. The blue color in (Figure 9) represents the graphical depiction of relative average water absorption.
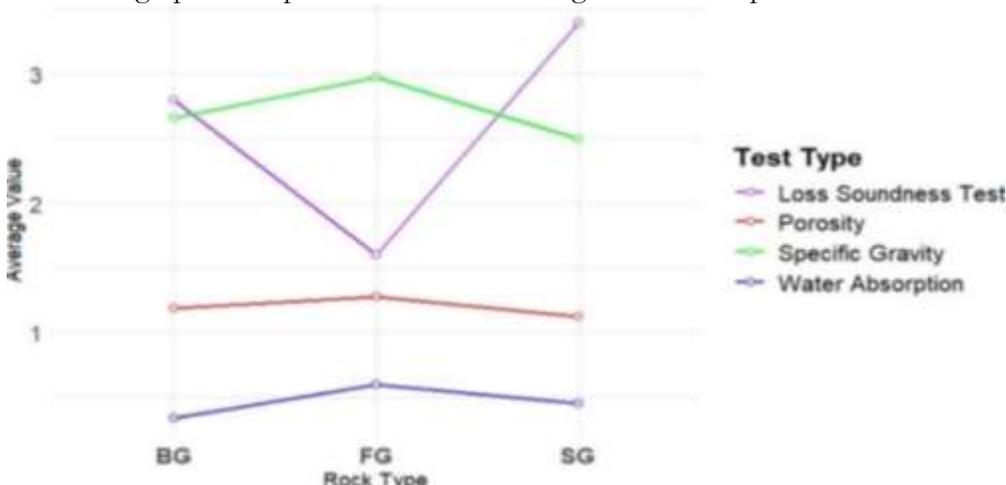
Figure 9. Results of Water Absorption, Specific Gravity, Porosity, and Soundness Test

Specific Gravity:

The average specific gravity values for the tested granites were recorded as Fulkin Granite (FG) 2.98, Bargen Granite (BG) 2.66, and Shing Granite (SG) 2.5. All mean values comply with the required specifications. According to ASTM C127, rocks with a specific gravity of ≥ 2.55 are deemed suitable for use as dimension stones. Therefore, all granite types tested are acceptable for use as dimension and building stones. Average specific gravity results of samples are presented in Table 4, while the green color in Figure 9 represents the average specific gravity values of the granites under study.

Porosity:

Bargen Granite (BG) recorded an average porosity of 1.19%, Fulkin Granite (FG) 1.28%, and Shing Granite (SG) 1.12%. Large grain size, the presence of cracks, and void spaces in granites contribute to higher porosity, which can reduce rock strength. All granites in this study have average porosity values that fall within the acceptable range for building materials and dimension stones. Figure 9 red shows the comparative mean porosity values of the granite types, and average results are presented in Table 4.

Soundness Test:

The maximum soundness test value was recorded for Bargen Granite (BG) 3.4, while the minimum was noted for Fulkin Granite (FG) 1.6 (see Table 4). These results indicate that all values fall within the acceptable limits specified by ASTM C88-90 (2003), making the granites suitable for construction use. Soundness tests assess resistance to chemical weathering, determining whether a rock is appropriate for use in roads and large-scale projects. The allowable limits are 18% for $MgSO_4$ and 12% for Na_2SO_4. Figure 9 purples present the average soundness test results.

Table 4 Physical test results for water absorption, specific gravity, porosity, and percentage loss soundness

Rock ID	Average water absorption.	Average Specific Gravity	Average Porosity	Average Loss soundness test
FG	0.60	2.98	1.28	1.6%
SG	0.45	2.5	1.12	3.4%
BG	0.34	2.66	1.19	2.8%

Discussion:

This study aimed to assess the engineering properties of granite samples collected from the Damote Valley in Gilgit, Pakistan. The results of petrographic, mechanical, and physical testing provide valuable insights into the characteristics of the granitic rocks and their potential use as dimension and construction stones.

The petrographic analysis of the granitic rocks from the Damote Valley indicates a complex mineralogical composition, with quartz, feldspar, plagioclase, mica (muscovite and biotite), and accessory minerals such as chlorite, apatite, and opaque minerals. The modal mineral content and grain size variations suggest that the granites fall within the granite compositional field on the IUGS classification diagram, consistent with their classification as coarse to medium-grained granites.

Notably, quartz content in the samples ranged from 25% to 43%, with strained quartz grains indicating significant deformation. This observation is crucial as strained quartz can impact the rock's mechanical properties, such as strength and durability. The presence of feldspar (both alkali feldspar and plagioclase) in varying amounts further contributes to the rock's overall strength, as feldspar minerals are generally strong and contribute to the rock's resistance to physical weathering.

The observed myrmakitic texture in alkali feldspar and the zoning in plagioclase grains further suggest that the granites have undergone complex geological processes, including partial

alteration and deformation. The presence of biotite and chlorite in some samples, as well as the poikilitic texture in feldspar grains, supports the hypothesis of a dynamic tectonic history for the region, which is consistent with the known geological history of the Kohistan Batholith.

The mechanical properties of the granite samples, including Unconfined Compressive Strength (UCS), Brazilian Tensile Strength (BTS), Schmidt Hammer Rebound, Ultrasonic Pulse Velocity (UPV), and Slake Durability, provide a comprehensive understanding of their strength and durability. The UCS values indicate that Bargain granite (BG) exhibits the highest compressive strength at 66.17 MPa, followed by Fulkin granite (FG) at 63.10 MPa, and Shing granite (SG) at 53.22 MPa. These values categorize the granites as moderately strong to strong, according to ISRM (1981). The high UCS in Bargain granite suggests its superior performance for structural applications where high compressive strength is critical, aligning with previous studies that show granites typically have UCS values 6–11 times higher than their tensile strengths.

The BTS values were also evaluated, with Bargain granite again showing the highest tensile strength at 12.04 MPa, followed by Fulkin granite at 12.04 MPa, and Shing granite at 7.55 MPa. All samples met the ASTM requirement for dimension and building stone use, which specifies a minimum BTS of 8.27 MPa. These findings underscore the suitability of these granite samples for construction, particularly in high-strength applications. Schmidt Hammer results, which measure rock surface hardness, revealed that Bargain granite had the highest rebound value (47), suggesting it has superior surface hardness compared to Fulkin (46) and Shing (43). This result correlates with the higher UPV values for Bargain granite, which recorded the highest velocity at 3218.6 m/s, suggesting better homogeneity and fewer voids or fractures compared to the other samples. The Slake Durability Index (SDI) values, ranging from 35.6% for Shing granite to 37.5% for Fulkin granite, indicate that all the granite samples exhibit moderate resistance to weathering and disintegration under wetting and drying conditions. While these values are below the maximum allowable limit of 40%, they demonstrate that the granites have sufficient durability for long-term use in environments subject to such cycles.

The physical properties of the granite samples, including water absorption, specific gravity, porosity, and soundness, further inform their suitability for construction applications. The water absorption values were low across all samples, with Fulkin granite showing the highest at 0.60%, followed by Shing granite at 0.45%, and Bargain granite at 0.34%. While Fulkin granite slightly exceeded the ASTM recommendation of 0.4%, all the samples remain within acceptable limits for dimension and construction stone. The differences in water absorption can be attributed to variations in mineral composition, grain size, and the presence of microfractures and voids in the rocks. Specific gravity values ranged from 2.5 to 2.98, typical for granitic rocks, indicating that all three granites are suitable for use as dimension stones. Fulkin granite, with the highest specific gravity of 2.98, is denser and may be stronger than the other samples. Shing granite, with the lowest specific gravity (2.5), could be less suitable for applications where weight is a concern. Porosity values, ranging from 1.12% to 1.28%, were low, indicating that the granites have good resistance to physical weathering and low water absorption potential. The soundness test results revealed that Bargain granite exhibited the highest resistance to chemical weathering, with a loss of 3.4%, followed by Shing granite (2.8%) and Fulkin granite (1.6%). These values demonstrate the good durability of all three granite samples against chemical weathering, making them suitable for use in construction projects exposed to variable environmental conditions such as temperature fluctuations and moisture changes.

Conclusion:

Based on the material characterization results, including petrography, water absorption, porosity, specific gravity, soundness, compressive strength, tensile strength, Schmidt hammer, point load index, and Slake durability, the following conclusions about the granite from the Damote Valley can be drawn.

- The granite exhibits a mineral composition primarily consisting of potassium feldspar, quartz, plagioclase, and mica, with secondary minerals such as chlorite and sericite.

- The granite demonstrates moderate to strong physio-mechanical properties, with water absorption and porosity values within acceptable ranges for dimension stone and construction materials.

- The average Uniaxial Compressive Strength (UCS) values of the granite from the Demote area are 63 MPa for Fulkin granite, 66 MPa for Bargain granite, and 53 MPa for Shing granite, indicating their suitability for engineering applications.

- The material shows consistent Schmidt hammer and point load index values across samples, suggesting homogeneity in mechanical performance.

- A correlation between specific mineralogical characteristics and mechanical behavior was identified, revealing that variations in texture and composition influence the granite's performance under stress.

Acknowledgment. Acknowledgments are considered necessary.

Author's Contribution. The corresponding author should explain the contribution of each co-author completely.

Conflict of interest. Authors are advised to explain that there exists no conflict of interest for publishing this manuscript in IJIST.

Project details. If this research was conducted as a result of a project, please give details like project number, project cost completion date, etc

References:

[1]   "(PDF) Tectonic subdivision of granitic rocks of north Pakistan." Accessed: Dec. 31, 2024. [Online].   Available: https://www.researchgate.net/publication/299826081_Tectonic_subdivision_of_granitic_rocks_of_north_Pakistan

[2]   M. T. George, N. B. W. Harris, and R. W. H. Butler, "The tectonic implications of contrasting granite magmatism between the Kohistan island arc and the Nanga Parbat-Haramosh Massif, Pakistan Himalaya," *Geol. Soc. Spec. Publ.*, vol. 74, pp. 173–191, 1993, doi: 10.1144/GSL.SP.1993.074.01.13.

[3]   M. P. Coward, M. Q. Jan, D. Rex, J. Tarney, M. F. Thirlwall, and B. F. Windley, "Geo-tectonic framework of the Himalaya of N Pakistan.," *J. Geol. Soc. London.*, vol. 139, no. 3, pp. 299–308, 1982, doi: 10.1144/GSJGS.139.3.0299.

[4]   J. L. P. Zeitler, R. A. Khan Tahirkheli, C. Naeser, N. Johnson, "Preliminary Fission Track Ages from the Swat Valley, Northern Pakistan," *J. Himal. Earth Sci.*, vol. 13, no. 1, pp. 63–65, 1980, [Online]. Available: http://ojs.uop.edu.pk/jhes/article/view/1184

[5]   L. Ahmad, M. T. Shah, and S. D. Khan, "Reflectance spectroscopy and remote sensing data for finding sulfide-bearing alteration zones and mapping geology in Gilgit-Baltistan, Pakistan," *Earth Sci. Informatics*, vol. 9, no. 1, pp. 113–121, Mar. 2016, doi: 10.1007/S12145-015-0239-X/METRICS.

[6]   I. Ahmed, M. Basharat, L. Sousa, and M. S. Mughal, "Evaluation of building and dimension stone using physico-mechanical and petrographic properties: a case study from the Kohistan and Ladakh batholith, Northern Pakistan," *Environ. Earth Sci.*, vol. 80, no. 22, pp. 1–17, Nov. 2021, doi: 10.1007/S12665-021-10007-Y/METRICS.

[7]   A. Hussain *et al.*, "Chemical composition of gemstones and characterization of their host pegmatites and country rocks from Chumar Bakhoor, Gilgit-Baltistan, Pakistan: implications for the source of gem-forming fluids," *Arab. J. Geosci.*, vol. 14, no. 13, pp. 1–15, Jul. 2021, doi: 10.1007/S12517-021-07682-3/METRICS.

[8]   M. K. A. Maqpoon, R.J.H., K. Khurshid, "Gilgit-Baltistan. Population," vol. 6, no. 7, p. 1,249,000, 2013,   [Online].   Available: https://www.pc.gov.pk/uploads/report/MICS_GB_1617-downloaded.pdf

[9]   J. A. Qureshi *et al.*, "Inventory and Quantitative Valuation of Geological and Geomorphological Sites from Gilgit-Baltistan, Northern Pakistan," *Geoheritage*, vol. 13, no. 4, pp. 1–15, Dec. 2021,

doi: 10.1007/S12371-021-00617-0/METRICS.

[10]   A. A. Q. Hannan Younis, Farooq Ahmad, Muhammad Anees, Atia Atiq, Nida Shakeel, Muhammad Adil, Khurram Mehboob, Abdulsalam M. Alhawsawi, Rashid Khan, Ahmed M. Khubrani and M. Ajaz, "Gamma radioactivity and Environmental radiation risks of Granitoids in Central and Western Gilgit-Baltistan, Himalayas, North Pakistan," *Results Phys.*, vol. 37, p. 105509, 2022, doi: https://doi.org/10.1016/j.rinp.2022.105509.

[11]   A. R. Asif, M. Sajid, W. Ahmed, and A. Nawaz, "Weathering effects on granitic rocks in North Pakistan: petrographic insights, strength classifications, and construction suitability," *Environ. Earth Sci.*, vol. 83, no. 11, pp. 1–28, May 2024, doi: 10.1007/S12665-024-11655-6/METRICS.

[12]   S. Mishra, A. Khetwal, and T. Chakraborty, "Physio-Mechanical Characterization of Rocks," *J. Test. Eval.*, vol. 49, no. 3, pp. 1976–1998, May 2021, doi: 10.1520/JTE20180955.

[13]   B. O. T. Zelealem Haftu , Nageswara Rao Cheepurupalli , , Yewuhalashet Fissha , Sri Chandrahas N, "Rock Mechanical Properties and Resource Potential of Dimensional Stone and Terrazzo in Tigray, Ethiopia: A Geological and Geomechanical Assessment," *Rock Mech. Lett.*, vol. 1, no. 1, p. 4, 2024, doi: https://doi.org/10.70425/rml.202401.4.

[14]   A. U. R. Syed Yasir Ali Shah, Dou Bin, Obaidullah , Javid Hussain, Khaleel Hussain, Ali Asghar, Hadi Hussain, "Physio-Mechanical Properties and Petrographic Analysis of NikanaiGhar Limestone KPK, Pakistan," *Open J. Civ. Eng.*, vol. 12, no. 2, pp. 169–188, 2022, doi: 10.4236/ojce.2022.122011.

[15]   M. B. Nadaf, V. Maralapalle, A. A. Zende, and A. I. A. Momin, "Mineralogical composition and strength characteristics of granite rocks," *Sadhana - Acad. Proc. Eng. Sci.*, vol. 49, no. 4, pp. 1–22, Dec. 2024, doi: 10.1007/S12046-024-02635-4/METRICS.

[16]   M. A. Alsaiari and A. A. El Aal, "Influence of composition on the physico-mechanical properties of granitic rocks used in floor covering and building cladding in Najran Region, Saudi Arabia," *Arab. J. Geosci.*, vol. 14, no. 20, pp. 1–18, Oct. 2021, doi: 10.1007/S12517-021-08387-3/METRICS.

[17]   "Evaluation of the durability of granite in architectural monuments - Google Search." Accessed: Dec. 31, 2024. [Online]. Available: https://www.google.com/search?q=Evaluation+of+the+durability+of+granite+in+architectural+monuments&oq=Evaluation+of+the+durability+of+granite+in+architectural+monuments&gs_lcrp=EgZjaHJvbWUyBggAEEUYOdIBBzU5MWowajeoAgCwAgA&sourceid=chrome&ie=UTF-8

[18]   A. R. Mahdi Askaripour,Ali Saeidi ,Patrick Mercier-Langevin, "A Review of Relationship between Texture Characteristic and Mechanical Properties of RockNo Title," *Geol. Surv. Finland. Rep. Investig.*, vol. 2, no. 1, pp. 262–296, 2022, doi: https://doi.org/10.3390/geotechnics2010012.

[19]   M. H. B. Nasseri and B. Mohanty, "Fracture toughness anisotropy in granitic rocks," *Int. J. Rock Mech. Min. Sci.*, vol. 45, no. 2, pp. 167–193, Feb. 2008, doi: 10.1016/J.IJRMMS.2007.04.005.

[20]   "(PDF) Petrography and physico-mechanical properties of the granitic rocks from Kumrat valley, Kohistan Batholith, NW Pakistan." Accessed: Dec. 31, 2024. [Online]. Available: https://www.researchgate.net/publication/275352897_Petrography_and_physico-mechanical_properties_of_the_granitic_rocks_from_Kumrat_valley_Kohistan_Batholith_NW_Pakistan

[21]   M. P. Searle, "Geological evidence against large-scale pre-Holocene offsets along the Karakoram Fault: Implications for the limited extrusion of the Tibetan plateau," *Tectonics*, vol. 15, no. 1, pp. 171–186, Feb. 1996, doi: 10.1029/95TC01693.

[22]   P. J. Treloar and C. N. Izatt, "Tectonics of the Himalayan collision between the Indian Plate and the Afghan Block: A synthesis," *Geol. Soc. Spec. Publ.*, vol. 74, pp. 69–87, 1993, doi: 10.1144/GSL.SP.1993.074.01.06.

[23]   M. Q. J. M. P. Searle, M. Asif Khan, J. E. Fraser, S. J. Gough, "The tectonic evolution of the Kohistan-Karakoram collision belt along the Karakoram Highway transect, north Pakistan," *Tectonics*, vol. 18, no. 6, pp. 929–949, 1999, doi: https://doi.org/10.1029/1999TC900042.

[24]   M. G. Petterson and P. J. Treloar, "Volcanostratigraphy of arc volcanic sequences in the Kohistan arc, North Pakistan: volcanism within island arc, back-arc-basin, and intra-continental tectonic settings," *J. Volcanol. Geotherm. Res.*, vol. 130, no. 1–2, pp. 147–178, Feb. 2004, doi:

10.1016/S0377-0273(03)00287-7.

[25]   M. T. Shah and J. W. Shervais, "The Dir-Utror metavolcanic sequence, Kohistan arc terrane, northern Pakistan," *J. Asian Earth Sci.*, vol. 17, no. 4, pp. 459–475, Aug. 1999, doi: 10.1016/S1367-9120(99)00009-7.

[26]   P. J. Treloar, M. G. Petterson, M. Q. Jan, and M. A. Sullivan, "A re-evaluation of the stratigraphy and evolution of the Kohistan arc sequence, Pakistan Himalaya: Implications for magmatic and tectonic arc-building processes," *J. Geol. Soc. London.*, vol. 153, no. 5, pp. 681–693, Sep. 1996, doi: 10.1144/GSJGS.153.5.0681.

[27]   J. V. M. A. Pêcher, L. Seeber, S. Guillot, F. Jouanne, A. Kausar, M. Latif, A. Majid, G. Mahéo, J. L. Mugnier, Y. Rolland, P. van der Beek, "Stress field evolution in the northwest Himalayan syntaxis, northern Pakistan," *Tectonics*, vol. 27, no. 6, 2008, doi: https://doi.org/10.1029/2007TC002252.

[28]   J. Ameratunga, N. Sivakugan, and B. M. Das, "Laboratory Rock Tests," pp. 207–223, 2016, doi: 10.1007/978-81-322-2629-1_9.

[29]   A. Aydin, "ISRM Suggested Method for Determination of the Schmidt Hammer Rebound Hardness: Revised Version," *ISRM Suggest. Methods Rock Charact. Test. Monit. 2007-2014*, pp. 25–33, 2008, doi: 10.1007/978-3-319-07713-0_2.

[30]   M. J. Le Bas and A. L. Streckeisen, "The IUGS systematics of igneous rocks," *J. Geol. Soc. London.*, vol. 148, no. 5, pp. 825–833, 1991, doi: 10.1144/GSJGS.148.5.0825.

[31]   M. Inoue and M. Ohomi, "Relation Between Uniaxial Compressive Strength And Elastic Wave Velocity of Soft Rock." OnePetro, Sep. 21, 1981. Accessed: Dec. 31, 2024. [Online]. Available: https://dx.doi.org/

[32]   B. H. G. Brady and E. T. Brown, "Rock Mechanics for underground mining: Third edition," *Rock Mech. Undergr. Min. Third Ed.*, pp. 1–628, 2006, doi: 10.1007/978-1-4020-2116-9/COVER.

[33]   A. Farhadian, E. Ghasemi, S. H. Hoseinie, and R. Bagherpour, "Prediction of Rock Abrasivity Index (RAI) and Uniaxial Compressive Strength (UCS) of Granite Building Stones Using Nondestructive Tests," *Geotech. Geol. Eng.*, vol. 40, no. 6, pp. 3343–3356, Jun. 2022, doi: 10.1007/S10706-022-02095-9/METRICS.